SUPPORTING INFORMATION

Synthesis and characterization of poly(vinylphosphonic acid-*co*-acrylic acid) copolymers for application in bone tissue scaffolds

Rebecca E. Dey,[†] Xia Zhong,[†] Peter J. Youle,[†] Qi Guang Wang,[‡] Ian Wimpenny,[§] Sandra Downes,[§] Judith A. Hoyland,[‡] David C. Watts,[‖] Julie E. Gough[§] and Peter M. Budd[†,]*

[†]School of Chemistry, University of Manchester, Manchester, M13 9PL, U.K.

[‡]Centre for Tissue Injury and Repair, Institute for Inflammation and Repair, Faculty of Medical and Human Sciences, University of Manchester, Manchester, M13 9PL, U.K.

[§]School of Materials, University of Manchester, Manchester, M13 9PL, U.K.

[‖]School of Dentistry and Photon Science Institute, University of Manchester, Manchester, M13 9PL, U.K.

1. Synthesis of PVPA-*co*-AA

With increasing initiator concentration, the yield and monomer conversion were found to increase. This was accompanied by a broad molecular weight distribution at an initiator concentration of 1.0 mol%. The synthesis was repeated to evaluate the reproducibility of the method. The results are presented in Table S1.

Table S1. Effect of initiator (AAPH) concentration on yield, monomer conversion, composition of copolymer, weight-average molar mass (M_w), number-average molar mass (M_n) and polydispersity (M_w/M_n), for copolymerization of vinyl phosphonic acid (VPA) with acrylic acid (AA). In each case, the monomer feed composition was 30 mol% VPA.

AAPH concentration (mol%)	Yield (%)	Monomer conversion (%)	VPA in copolymer (mol%)	M_w (g mol^{-1})	M_n (g mol^{-1})	M_w/M_n
0.1	74	89	22	267100	29900	8.93
0.1	73	86	24	284600	34800	8.18
0.3	84	92	22	195400	26500	7.37
0.3	78	93	26	145000	18600	7.78
1.0	93	96	23	159400	12400	12.9
1.0	95	98	16	142000	13600	10.4

2. Characterization of PVPA-*co*-AA

2.1 Gel Permeation Chromatography (GPC)

Molecular weight distributions from GPC are shown in Figure S1.

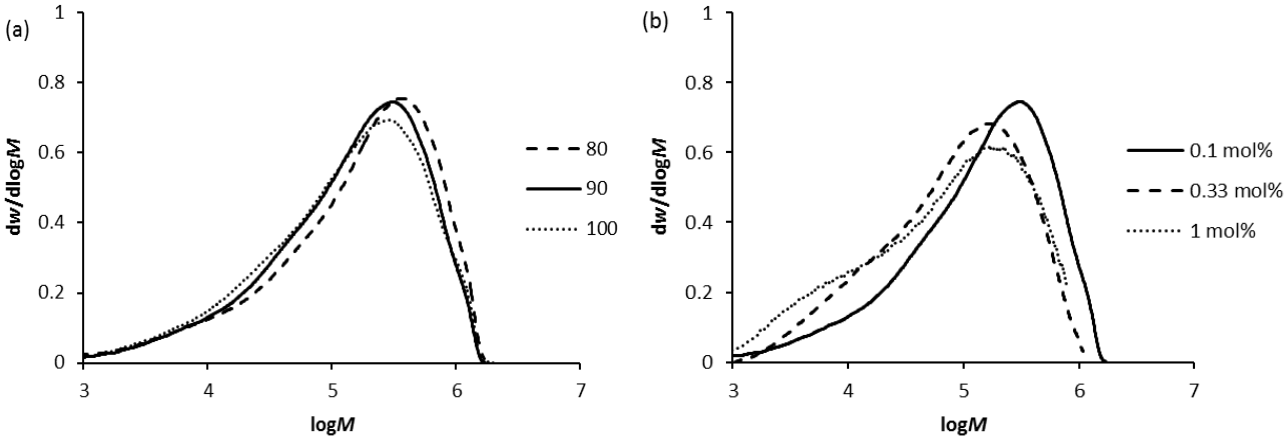

Figure S1. Molecular weight distributions for PVPA-*co*-AA, with a feed ratio of 30 mol% VPA, for (a) initiator concentration of 0.1 mol% and temperatures of 80, 90 and 100 °C, and (b) a temperature of 90 °C and initiator concentrations of 0.1, 0.33 and 1 mol%.

2.2 Elemental analysis

Elemental analysis data from ICP-MS are shown in Table S2.

Table S2. Elemental analysis of PVPA-*co*-AA samples with different feed compositions.

Sample Code	Monomer feed ratio (VPA:AA)	C (%)	H (%)	P (%)
PVPA-0	0:100	46.3	5.8	-
PVPA-20	20:80	42.2	5.8	4.1
PVPA-30	30:70	37.0	5.3	9.3
PVPA-40	40:60	33.1	5.3	11.1
PVPA-60	60:40	27.6	5.2	18.3
PVPA-80	80:10	22.6	4.9	22.7
PVPA-100	100:0	19.8	4.6	26.1

The mole ratio, $r_{P/C}$, of P to C in the copolymer was calculated from the elemental analysis data using equation S1.

$$r_{P/C} = \frac{\%P \times M_C}{\%C \times M_P} \qquad (S1)$$

where M_C is the molar mass of carbon and M_P is the molar mass of phosphorus. The mole fraction, x_{VPA}, of VPA in the copolymer was then calculated using equation S2.

$$x_{VPA} = \frac{1}{1 + (\frac{1 - 2r_{P/C}}{3r_{P/C}})} \qquad (S2)$$

The molar mass of a hypothetical monomer (M_m) was calculated using equation S3.

$$M_m = (M_{VPA} \times x_{VPA}) + (M_{AA} \times x_{AA}) \qquad (S3)$$

where M_{VPA} and M_{AA} are the molar masses of VPA and AA, respectively, and x_{VPA} and x_{AA} are the mole fractions of VPA and AA in the copolymer. The degree of neutralization (α) is defined as the equivalents of base added per acid group, shown in equation S4.

$$\alpha = \frac{n_{OH^-}}{n_{H^+}} \qquad (S4)$$

where n_{OH^-} is the moles of base added and n_{H^+} is the moles of acid groups in the copolymer, determined by dividing the mass of polymer by M_m.

2.3 FT-IR spectroscopy

Figure S2 shows the FT-IR spectra of PVPA-60 and PVPA-80, which were not included in Figure 3 of the paper. There is an increase in the intensity of the P-O-H bands, which can be seen at 985-905 cm^{-1}, as the VPA content in the copolymer is increased. This is accompanied by a decrease in the C=O band of the carboxylic acid group, which appears at 1696 cm^{-1}.

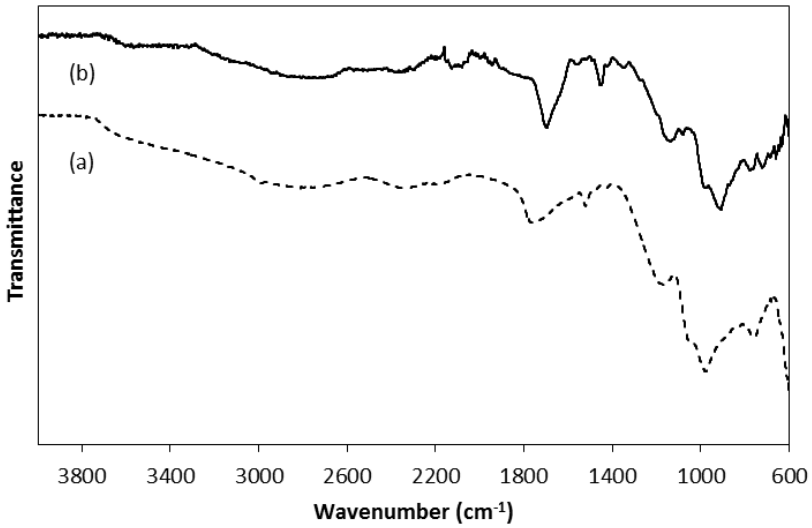

Figure S2. FT-IR spectrum of (a) PVPA-80 and (b) PVPA-60.

3. Monomer reactivity ratios of AA and VPA

Monomer reactivity ratios were calculated by applying the copolymer equation S5, developed by Mayo and Lewis.[1]

$$\frac{\mathrm{d}[\mathrm{M}_1]}{\mathrm{d}[\mathrm{M}_2]} = \frac{[\mathrm{M}_1](r_1[\mathrm{M}_1] + [\mathrm{M}_2])}{[\mathrm{M}_2]([\mathrm{M}_1] + r_2[\mathrm{M}_2])} \qquad \text{(S5)}$$

where $[M_1]$ and $[M_2]$ are the concentrations of monomer 1 and monomer 2, and r_1 and r_2 are their reactivity ratios.

A range of copolymers was produced with varying composition and their characterization data are summarised in Table S3. The reactions were carried out to low conversion so as to minimize unequal monomer consumption throughout the course of the reaction. The compositions 80:20 and 90:10 (AA:VPA) had too high conversions to be included in the study.

Table S3. Feed and copolymer compositions (AA:VPA), conversion, yield and weight-average molar mass (M_w), number-average molar mass (M_n) and polydispersity (M_w/M_n) for the synthesis of PVPA-*co*-AA to low conversion.

Feed Composition (*f*)	Copolymer Composition (*F*)	Monomer Conversion (%)	Yield (%)	M_w (g/mol)	M_n (g/mol)	M_w/M_n
10:90	60:40	2.9	17	-	-	-
20:80	63:37	4.8	19	4194	2467	1.7
30:70	73:27	7.4	16	17343	5456	3.179
40:60	80:20	12.3	42	50725	11309	4.486
50:50	86:14	17.4	41	122303	20530	5.957
60:40	89:11	20	67	153197	28462	5.231
70:30	91:9	32.9	54	180617	37969	4.757
80:20	94:6	54.3	70	-	-	-
90:10	96:4	64.5	78	-	-	-

Monomer reactivity ratios were evaluated using linear fitting methods such as that of Fineman and Ross,[2] shown in equation S6.

$$G = r_1 H + r_2 \qquad \text{(S6)}$$

Where G is defined as $X(Y\text{-}1)/Y$ and H as X^2/Y. X is f_1/f_2 (feed ratio) and Y is F_1/F_2 (copolymer ratio). A plot of G versus H allows r_1 to be calculated from the slope and r_2 from the intercept. The more accurate linearization method developed by Kelen and Tüdos[3] is shown in equation S7.

$$\eta = \left[r_1 + \frac{r_2}{\alpha}\right]\xi - \frac{r_2}{\alpha} \qquad \text{(S7)}$$

where η is equal to $G/(\alpha+H)$ and ξ is equal to $H/(\alpha+H)$. A plot of η versus ξ yields a straight line with $-r_2/\alpha$ and r_1 as the intercept when extrapolating to ξ = 0 and ξ = 1, respectively. The α parameter corresponds to $(Y_m \times Y_M)^{1/2}$ and corrects for the minimum (Y_m) and maximum (Y_M) values of Y, which, when using Fineman-Ross, can lead to differing r values depending on the choice of M_1 and M_2. In this study, AA was chosen as M_1 and VPA as M_2. The parameters used for both methods are presented in Table S4.

Table S4. Parameters for the Fineman-Ross and Kelen-Tüdos[a] methods.

f	F	X	Y	H	G	ξ	η
10:90	60:40	0.10	1.500	0.007	0.030	0.002	0.008
20:80	63:37	0.25	1.703	0.037	0.103	0.009	0.026
30:70	73:27	0.43	2.704	0.068	0.270	0.017	0.068
40:60	80:20	0.60	4.000	0.090	0.450	0.023	0.113
50:50	86:14	1.00	6.143	0.163	0.837	0.040	0.206
60:40	89:11	1.50	8.091	0.278	1.315	0.067	0.315
70:30	91:9	2.30	10.11	0.523	2.073	0.119	0.469

[a] α is 3.894.

Figure S3 shows the Fineman-Ross and Kelen-Tüdos plots for evaluation of the reactivity ratios of VPA and AA.

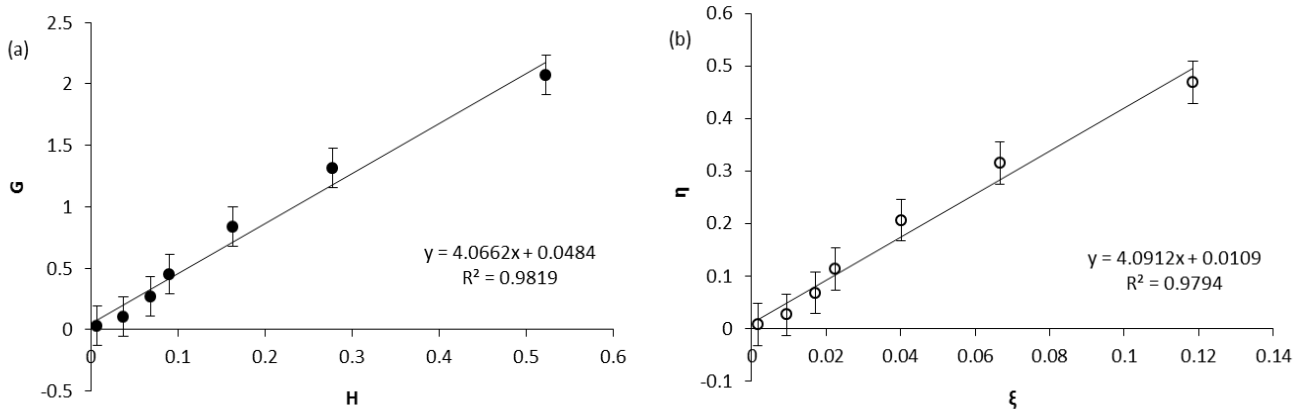

Figure S3. (a) Fineman-Ross plot and (b) Kelen-Tüdos plot for the evaluation of the monomer reactivity ratios of VPA and AA.

4. Calcium chelation calibration

The calibration curve for the determination of calcium chelation by PVPA-*co*-AA is shown in Figure S4. The oxidation-reduction potential (ORP) of Ca^{2+} is plotted against the logarithm of $CaCl_2$ concentration.

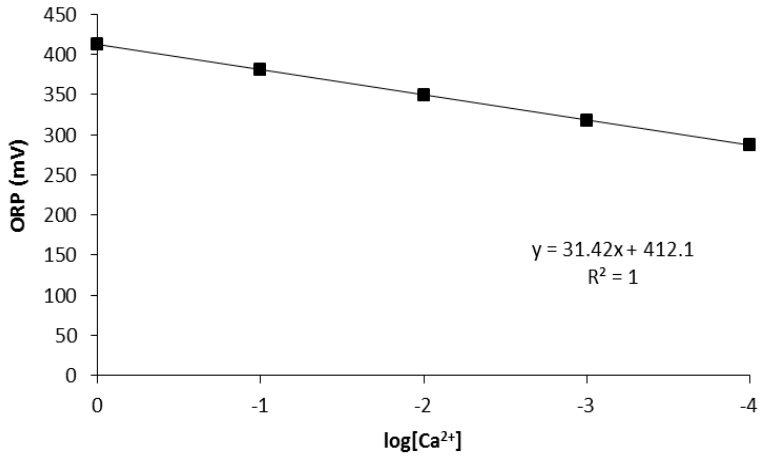

Figure S4. Calibration curve for the determination of calcium chelation by PVPA-*co*-AA.

0.1 M $CaCl_2$ was added to solutions of PVPA-*co*-AA and the free calcium concentration was calculated using the calibration curve and equation S8.

$$[Ca^{2+}]_{free} = 10^{\frac{ORP-412.1}{31.42}} \qquad (S8)$$

The calcium chelation was then calculated by subtracting the free Ca^{2+} measured from the total Ca^{2+} added.

5. Rheology of PVPA-*co*-AA-calcium complexes

PVPA-30 was dissolved in deionized water (10 mg mL^{-1}) and the pH was adjusted to 7.3 using 0.1 M NaOH. $CaCl_2$ was then added to the polymer solution (0.01, 0.05, 0.1, 0.5 or 1 M). Rheological measurements were performed using a thermostated, oscillating rheometer (Ares LN2, TA Instruments, Hertfordshire) at 20.0°C with parallel plate geometry (plate diameter 50 mm, gap 0.051 mm). The strain was set at 200% with a frequency of 1 Hz, i.e. in the linear viscoelastic region. Tests were performed in triplicate. Analysis was performed using the manufacturer's supplied software (TA Data Analysis, TA Instruments).

Figure S5 shows the change in dynamic viscosity with shear rate, for aqueous solutions of PVPA-30 (10 mg mL^{-1}) with different concentrations of added calcium chloride. There is a decrease in viscosity with increasing salt concentration, as typically observed for polyelectrolytes. This may be attributed to a conformational change of the polymer. This occurs via a non-specific interaction whereby the divalent ions can screen the electrostatic repulsions and thus reduce the electrical double layer. Alternatively, because PVPA-*co*-AA has a high affinity for calcium ions, a chemical association may take place, which induces ionic crosslinks within the polymer.[4]

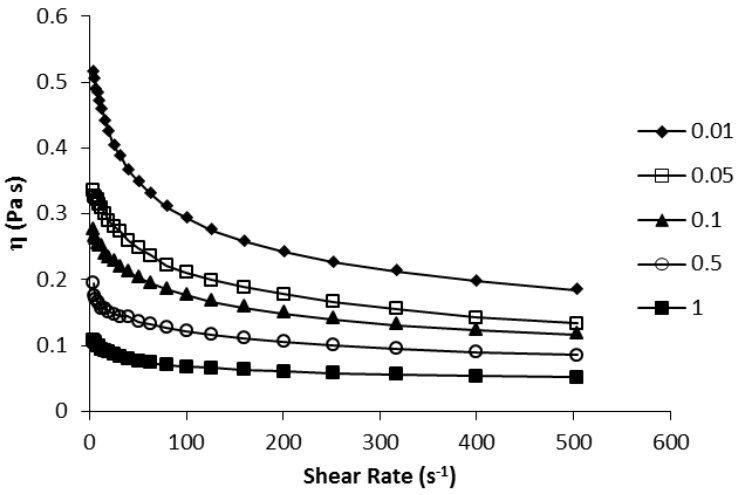

Figure S5. Dependence of dynamic viscosity on applied shear rate for aqueous solutions of PVPA-30 (10 mg mL^{-1}) with calcium chloride at concentrations of 0.01 (◆), 0.05 (□), 0.1 (▲), 0.5 (○) and 1 (■) M.

6. Zeta potential of PVPA-*co*-AA-calcium complexes

PVPA-30 was dissolved in deionized water (10 mg mL^{-1}) and the pH was adjusted to 7.3 using 0.1 M NaOH. $CaCl_2$ was then added to the polymer solution (0.01, 0.05, 0.1, 0.5 or 1 M). The solutions were filtered through mixed ester membrane filters (Millex-GS, Merck Millipore, Hertfordshire) with a pore size of 0.22 μm. Each sample was filtered into a disposable capillary cell (DTS1070, Malvern, Worcestershire). The zeta potential measurements were performed on a Malvern Zetasizer Nano-ZS instrument.

The binding of calcium ions to the negatively-charged groups of PVPA-*co*-AA reduces the effective charge of the polymer. This has been proven by measuring the zeta potential of aqueous solutions of PVPA-30 (10 mg mL^{-1}) with increasing calcium concentration (Figure S6). The zeta potential becomes less negative with increasing calcium concentration and thus

the stability decreases. Above concentrations of 0.1 M Ca^{2+}, a hydrophobic complex forms and the polymer precipitates out of solution.

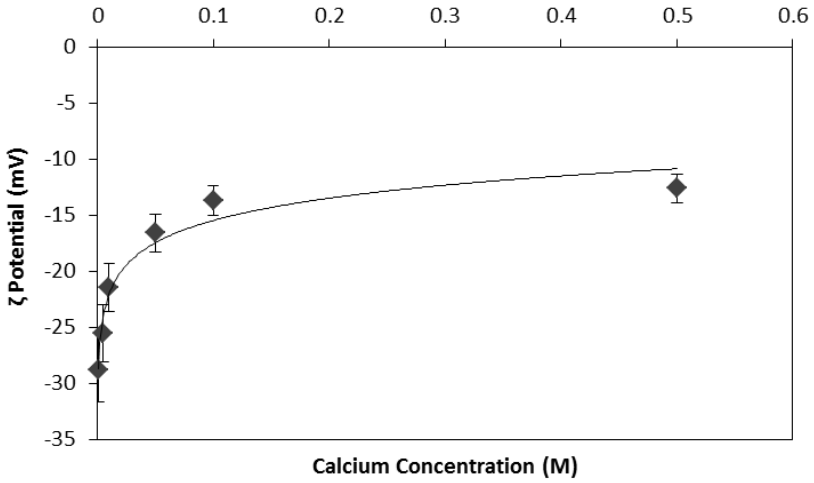

Figure S6. Dependence of zeta potential on calcium chloride concentration for aqueous solutions of PVPA-30 (10 mg mL^{-1}).

7. Assessment of cell metabolic activity for VPA and AA

Figure S7(a-c) shows the fold change in cell metabolic activity as a function of concentration for VPA and AA monomers at 0, 24 and 72 h time points. The results indicate that, compared with a phosphate buffer solution (PBS) control, AA and VPA monomers, with concentrations ranging from 1-500 μM, had no detrimental effect on SaOS-2 cell metabolic activity in a 72 h culture period.

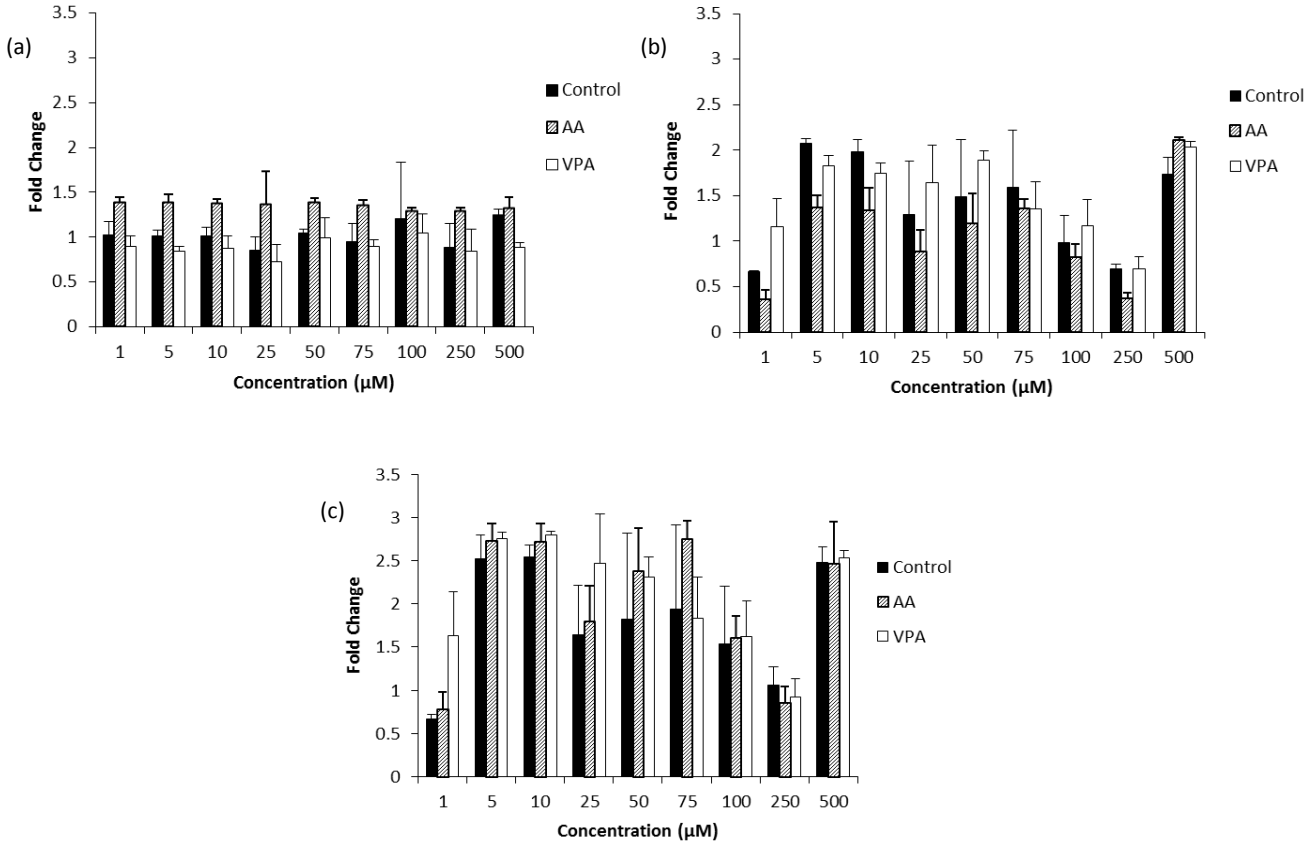

Figure S7. Determination of cell metabolic activity for AA and VPA monomers at (a) 0 h, (b) 24 h and (c) 72 h time points, for a range of monomer concentrations, compared with a PBS control.

Figure S8 shows the fold change in cell metabolic activity for AA (0.36 µg mL^{-1}) and VPA (0.54 µg mL^{-1}) monomers over a 72 h culture period. The results indicate that, at these concentrations, AA and VPA had no detrimental effect on SaOS-2 cell metabolic activity. The difference between the control and AA and VPA monomers is not statistically significant at any time point.

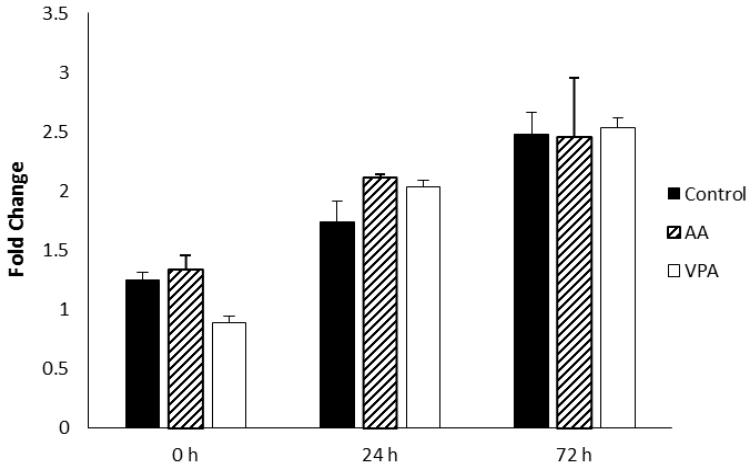

Figure S8. Determination of cell metabolic activity up to 72 h, for molar concentrations of monomer of 500 μM, corresponding to weight concentrations of 0.36 and 0.54 μg mL^{-1} for AA and VPA, respectively, compared with a PBS control.

REFERENCES

1. Mayo, F. R.; Lewis, F. M., *J. Am. Chem. Soc.* **1944,** *66*, 1594-1601.
2. Fineman, M.; Ross, S. D., *J. Polym. Sci.* **1949,** *5*, 259-265.
3. Kelen, T.; Tüdos, F., *J. Macromol. Sci. Chem.* **1975,** *9*, 1-27.
4. Olvera de la Cruz, M.; Belloni, L.; Delsanti, M.; Dalbiez, J. P.; Spalla, O.; Drifford, M., *J. Chem. Phys.* **1995,** *103*, 5781-5791.